Automated Detection of the Intercommissural Line for Stereotactic Localization of Functional Brain Images

Satoshi Minoshima, Robert A. Koeppe, Mark A. Mintun,* Keven L. Berger, Stephan F. Taylor, Kirk A. Frey and David E. Kuhl

Division of Nuclear Medicine, Department of Internal Medicine and Department of Psychiatry, University of Michigan, Ann Arbor, Michigan

A technique has been developed for automated detection of the intercommissural (AC-PC) line for positron emission tomography (PET). The AC-PC line is estimated from the location of four internal landmarks: the frontal and occipital poles, the inferior aspect of the anterior corpus callosum, and the subthalamic point. The landmarks are detected automatically in PET mid-sagittal slices by combining edge detection, interpolation and profile curve analysis techniques. The anatomical relationship between the true and estimated AC-PC lines from the landmarks was confirmed by analysis of magnetic resonance (MR) images. Accuracy of the automated estimation technique was assessed in co-registered PET and MR images, which showed minimal angular differences and displacements of the estimated from the true AC-PC lines. The automated detection of the AC-PC line in a PET study enables accurate stereotactic localization of functional signals without the need for additional anatomical imaging and provides a basis for objective and reproducible intersubject comparison.

J Nucl Med 1993; 34:322–329

Anatomical localization of functional signals is an essential aspect of data analysis in positron emission tomography (PET) (*1,2*). For a single subject, functionally-altered areas in the brain need to be interpreted with precise anatomical localization of the PET signal. For groups of subjects, intersubject data analysis usually requires comparison of functional activities of corresponding areas in the brain, which should be determined by an objective and reproducible anatomical localization method. A common approach reported for addressing these needs has been the use of an anatomical image from the same subject as a reference image (*3–8*). Both magnetic resonance (MR) imaging and x-ray computed tomography

(CT) can be employed for this purpose. Accurate co-registration between PET and the anatomical reference image is crucial for this approach (*3,5–9*).

Another approach is to align PET images to a standard orientation that indirectly enables anatomical localization. This indirect localization is especially useful when structures of the brain cannot be directly identified in an image. An atlas based on the standard orientation can be used as an anatomical reference to localize the signals in a standard orientation (*10*). Head alignment according to the cantho-meatal (CM) or orbitomeatal (OM) lines is an example of this approach, providing standard anatomical orientation among the subjects. However, the CM and OM lines are determined by bony structures of the head and do not necessarily provide accurate orientation of the brain (*11*). Instead, the line which passes through the anterior and posterior commissures of the brain (the AC-PC line) has been reported to enable more consistent and accurate localization of brain structures (*11–15*). Once a set of brain PET images has been aligned to a stereotactic coordinate system according to the AC-PC line, a standard stereotactic atlas (*12,13*) or a customized stereotactic atlas (*16*) can be used to localize PET signals.

To determine the AC-PC line for a PET study, individual lateral skull x-rays (*5,17*) as well as head fixation devices (*18,19*) have been used. Alternatively, Friston et al. (20) have described a method for the direct estimation of the AC-PC line from PET images. This method requires subjective identification of four internal landmarks from a PET image set to estimate the AC-PC line. We have implemented this method in our laboratory and found that visual identification of some brain structures in a PET image, such as the hippocampus and the superior edge of the anterior cingulate gyrus, was often ambiguous. Identification of the landmarks required visual inspection by persons with expertise in brain anatomy and PET imaging. Both intra- and interobserver differences were found to be substantial.

To remove ambiguity inherent in subjective identification of these landmarks, we have developed an automated technique for estimating the AC-PC line which identifies

four landmarks within the PET images: the frontal pole point of the brain (FP), the inferior aspect of the anterior corpus callosum (CC), the subthalamic point (TH) and the occipital pole point (OP). The FP and OP have been reported to provide good estimates of the AC-PC line (*11*). The TH resides on the AC-PC line since this line separates the thalamus from the subthalamic region (*13*). The CC is located approximately on the AC-PC line in a stereotactic coordinate system (*13*) and is easily placed on a distinct gray-white matter border. Advantages of the automated method include objectivity, reproducibility, and the capability to process large numbers of subjects. In this study, we describe an algorithm for the automated detection of the four landmarks, anatomical validation of the estimated AC-PC lines in MR scans, and accuracy of the automated AC-PC line estimation in PET images.

MATERIALS AND METHODS

Automated Detection of PET Landmarks

To estimate the AC-PC line from a PET image set, four landmarks, FP, CC, TH, and OP, are automatically detected in sagittal slices of a PET image set. Details of the algorithm are described in the Appendix and shown in Figure 1. Briefly, the CC point is defined as the most anterior ventral aspect of the corpus callosum, located on the gray-white matter border between the anterior corpus callosum and the cingulate gyrus (Fig. 1C). The OP is defined as the most posterior point of the brain and detected on the posterior edge of the brain at greatest distance from the CC (Fig. 1D). The FP is defined as the most anterior point of the brain, located on the anterior edge of the brain as the furthest point from the OP (Fig. 1D). The TH is defined as the inferior point of thalamus and detected by application of a cutoff threshold to thalamic activity (Fig. 2). The AC-PC line is estimated on the basis of these four points by simple linear regression (Fig. 3). The center of the AC-PC line is defined as the midpoint between the anterior and posterior edges of the brain in the mid-sagittal slice.

To detect these landmarks, multiple estimates of landmarks are necessary to avoid a bias caused by the initial brain orientation within the image matrix. First, the approximate OP is determined as the most posterior point of the brain in the midsagittal contour image (Fig. 1B). Next, the approximate CC is defined as the most ventral point along the gray-white border of the inferior aspect of the anterior corpus callosum (Fig. 1C) on a tangential line originating from the approximate OP. These two points are affected by the initial brain orientation in the image matrix, and thus their estimates require a second iteration. The final OP is detected on the posterior edge of the brain as the furthest point from the approximate CC (Fig. 1D). Since the inferior aspect of the corpus callosum is usually restricted to a small area (Fig. 1C), the approximate CC is always close to the final CC, and therefore location of the *final* OP is not affected by the initial brain orientation. Although a displacement between the approximate OP and the final OP is usually small, the final CC is re-defined as the most ventral point of the gray-white matter border on a tangential line originating from the final OP.

Implementation of the Algorithms

The automated program, which includes application of preprocessing steps (see Appendix) to the PET image set, was written
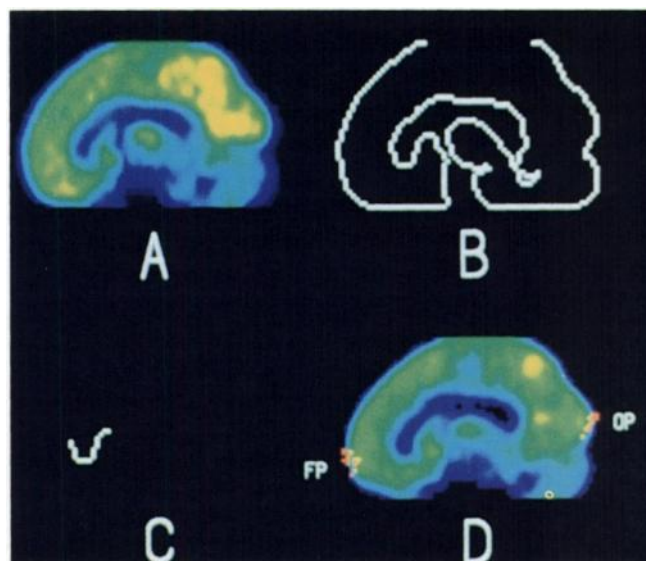

FIGURE 1. Detection of the landmarks. (A) Averaged mid-sagittal slice for detection of the CC point. (B) Contour image after edge detection and segmentation. (C) Gray-white matter border between inferior aspect of the anterior corpus callosum and the anterior cingulate gyrus. (D) Detected OP and FP points. To demonstrate the detection of the OP and FP, all detected points in the algorithm are shown simultaneously in a mid-sagittal slice. Since the OP and FP points are detected by 0.1 pixel steps, each point is displayed to the nearest pixel.

in C language and implemented on a SUN SPARC station (Sun Microsystems, Mountain View, CA). The program creates stereotactic transformation parameters and a mid-sagittal image with the estimated AC-PC line. These parameters indicate the center coordinates and slope of the AC-PC line in a PET image set, but are also available for further image processing. Visual inspection of the mid-sagittal image with the estimated AC-PC line insures that the algorithm does not generate grossly anomalous results (Fig. 3).
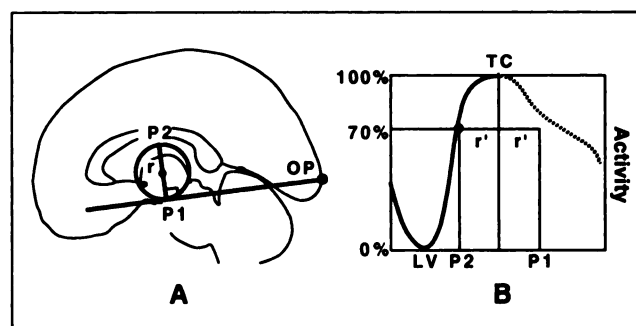

FIGURE 2. Detection of the subthalamic point TH. (A) Definition of the two points, P1 and P2. P1 is a point of contact between a tangential line originating from the OP and an imaginary circle with a radius r and a center corresponding to the approximate thalamic center. P2 is a diametrically opposite point to P1 on the imaginary circle. (B) Profile activity curves at the P2 with various radius r. The TH is determined by the P1 that corresponds to the P2 at 70% of the peak thalamic value (TC) above the lowest ventricular value (LV) (radius at r').
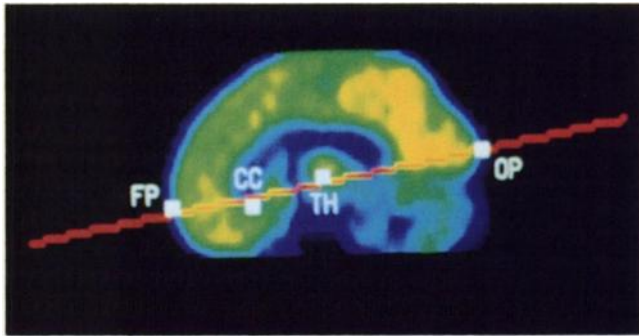
FIGURE 3. Estimated AC-PC line superimposed in a mid-sagittal slice. White dots indicate detected landmarks. Approximate accuracy of the estimation can be assessed visually in this image.

PET and MR Scans

To test and validate the method, [^{18}F]-2-fluoro-2-deoxy-D-glucose (FDG) PET images were collected from seven subjects (age 33 ± 9 yr, mean ± s.d.) whose anatomical structure as measured by a mid-sagittal slice in an MR image was judged to be normal by a radiologist. Studies were performed using a Siemens 931/08-12 scanner (CTI Inc. Knoxville, TN), which collects 15 simultaneous slices with a slice-to-slice separation of 6.75 mm (21). Each subject's head was carefully aligned in the gantry using laser beam guides in planes of the cranial midline and the CM line. Two sequential interleaved scan sets, total 60 million counts/set, were acquired 30 min after intravenous injection of 10 mCi of FDG. The images were reconstructed with a Shepp filter with a cutoff frequency of 0.35 cycles per projection (projection spacing 2.36 mm) and attenuation corrected with ellipse fitting, giving a reconstructed in-plane FWHM 7.0–7.5 mm and axial resolution 7.0–8.0 mm. While two interleaved scans were collected, only the first scan was used in the following validations of the method because we wished to test this routine as it would be applied to any type of study routinely performed in our laboratory (i.e., ^{15}O-water imaging with a bolus injection, dynamic receptor imaging) that has only 15 slices simultaneously acquired.

Two MR image types were used to validate the method. First, sequential transverse images (repetition time (TR) = 500 ms, echo time (TE) = 20 ms, 256 × 256 matrix, 5 mm thickness) covering the whole brain were obtained from the same seven subjects using a GE Signa 1.5 tesla imaging system (General Electric Co., Milwaukee, WI). Each volume image of the brain was resized and aligned into the orientation of the corresponding PET image with an adaptation of the user-interactive method of Pietrzyk and co-workers (22). Errors of co-registration in this routine are reported to be within 2–4 mm. Second, sets of sagittal slices (TR = 600 ms, TE = 15 ms, 256 × 192 matrix, 5 mm thickness) were collected from 18 subjects (age 33 ± 11 yr) whose gross anatomical structures in midsagittal slices were confirmed to be normal by two radiologists.

Anatomical Relationship Between the True and Estimated AC-PC Lines in MR Scans

In order to confirm the anatomical relationship between the true AC-PC line and its estimate from the landmarks, we identified the true AC-PC line as the line passing through the superior

edge of the anterior commissure and the interior edge of the posterior commissure (13) as well as the four landmarks, FP, CC, TH, and OP, on each of the 18 sagittal MR images. The four landmarks were placed manually in sagittal slices according to their definitions. The OP and FP were determined by measuring the longest distance from the CC and OP, respectively. The AC-PC line was estimated from those four landmarks by simple linear regression and placed on the mid-sagittal slice (Fig. 4). The center point of the true AC-PC line was calculated as the mid-point between the anterior and posterior commissures on the true AC-PC line (12). A center point of the estimated AC-PC line was calculated as the mid-point of the anterior and posterior edges of the brain on the estimated AC-PC line. The true and estimated AC-PC lines were compared in each subject in terms of the angular difference between the lines and horizontal and vertical displacements of the centers (Fig. 5). A positive angular difference denotes the anterior convergence of the lines. The horizontal displacement was expressed as the percentage of the anteroposterior length of the brain. The vertical displacement was expressed as the percentage of the brain height, determined as the length between the true AC-PC line and the top of the brain. Positive values of the horizontal and vertical displacements denote posterior and dorsal displacements of the estimated center, respectively.

Validation of the Automated Method

To assess the accuracy of the automated estimate of the AC-PC line in a PET study, we used co-registered PET and MR scans from seven subjects. First, we applied the automated method to a PET image to estimate the AC-PC line. Then, the true AC-PC line was determined from the co-registered MR image. Comparison of the estimated AC-PC line from PET and the true AC-PC line from the co-registered MR image enables a direct assessment of the accuracy of the automated method. Angular differences as well as horizontal and vertical displacements of the centers of the two lines were evaluated in the same manner as described in the previous section. To assess the accuracy of detecting each land-
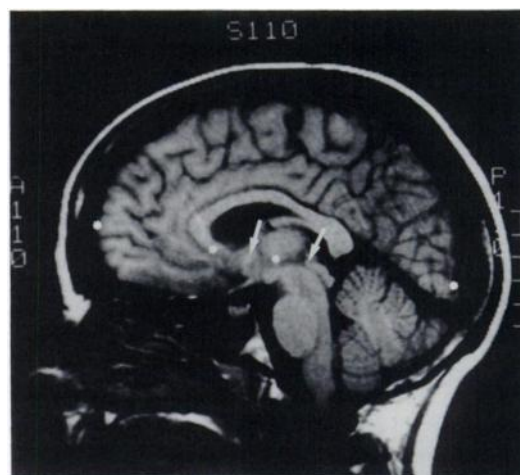

FIGURE 4. Anatomical relationship between the two commissures (arrows) and the four landmarks (asterisks) in a mid-sagittal MRI. The true AC-PC line is defined as a line passing through the superior edge of the anterior commissure and the inferior edge of the posterior commissure. The estimated AC-PC line is determined by simple linear regression from the four landmarks.
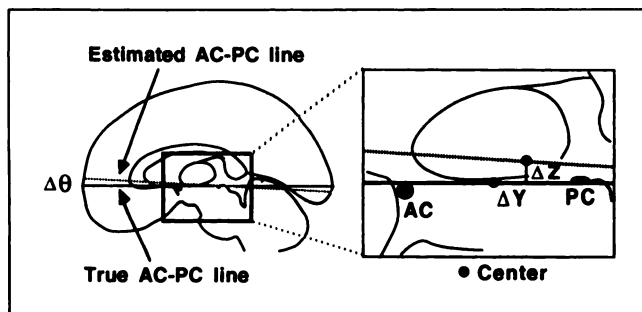
FIGURE 5. Validation of the estimated AC-PC line. $\Delta\theta$ = angular difference, ΔY = horizontal displacement, ΔZ = vertical displacement, AC = the anterior commissure and PC the posterior commissure.

mark by the automated method, the mean and standard deviation of the vertical displacement of the detected landmark from the true AC-PC line were calculated for each point. Displacements were expressed as the percentage of the brain height. Positive values indicated dorsal displacement to the true AC-PC line.

Comparison with Manual Methods

By using the same sets of co-registered PET and MR scans, we compared the accuracy of the automated method with two manual methods. First, we applied the method of Friston et al. (20), which uses a different set of four landmarks, manually placed, to a PET image set to estimate the AC-PC line. Second, we manually placed the proposed landmarks used in our method, FP, CC, TH and OP, on a mid-sagittal PET slice using an interactive program to estimate the AC-PC line. The CC, TH, OP and FP were placed in this order. To avoid bias from the interhemispheric space and to include the true frontal and occipital poles as well as the entire activity of the thalamus, the mid-sagittal slice was created by averaging resliced sagittal slices through the middle one-third of the brain. Both manual methods were applied twice for each subject without previous information of the estimated lines. The estimated AC-PC lines were averaged over the two trials for each subject and compared with the true AC-PC lines in the MR images, as described above. The angular difference and the center displacements for each method were statistically compared using analysis of variance (ANOVA) and Bartlett's test (23). In both statistical procedures, p ≤ 0.05 was considered significant.

Effect of PET Image Resolution

Since the automated method may be applied to various functional images reconstructed by different filter functions and of differing intrinsic contrast, we evaluated the effect of the image spatial resolution on estimation of the AC-PC line. A neighborhood averaging filter (24) of N × N pixels (N = 3, 5, 7, ... 13) was applied to blur each slice of the PET image. The automated method was applied to the blurred image sets and the estimated AC-PC lines were compared with the true AC-PC lines determined from the co-registered MR scans, as described previously.

Stereotactic Localization Using the Automatically Estimated AC-PC Line

The accuracy of stereotactic localization using the automatically detected PET AC-PC line was assessed by mapping two major sulci from co-registered MR images into the stereotactic

proportional system. The AC-PC lines were estimated by the automated method in the seven corresponding PET images. The location in the central sulcus was identified and traced in resliced sagittal and transverse planes of the co-registered MR image by referring to true locations of the anterior and posterior commissures. The sagittal and transverse slices were helpful in identifying superior and inferior parts of the central sulcus, respectively. The parieto-occipital sulcus was easily identified in the paramedian sagittal slices (25). In each hemisphere of the seven subjects, five to eight points along both the central sulcus on the lateral surface of the brain and the parieto-occipital sulcus were identified. Coordinates of the detected points were transformed into the stereotactic proportional system according to the estimated AC-PC line in the PET image. Brain height, width, and anteroposterior length were measured in the MR image to adjust the individual brain dimensions to the proportional system by simple linear transformation. The transformed points were interpolated to show the approximate location of the central sulcus. Fourteen estimated sulci were displayed in a lateral view of the stereotactic proportional system (13) and the distribution of the estimated central sulci was compared with a standard location of the central sulcus in the stereotactic system. Also, three to four points along the parieto-occipital sulcus were identified in a mid-sagittal plane, processed in the same manner and displayed simultaneously in the lateral view of the stereotactic system.

RESULTS

Validation of the Estimated AC-PC Line from the Four Landmarks in MR Scans

The estimation of the AC-PC line from four landmarks was validated in 18 MR images. The mean vertical displacement between centers of the true and estimated AC-PC lines was 0.8% ± 1.5% (mean ± s.d.) of the brain height and the estimated center located dorsally to the true AC-PC line. The mean horizontal displacement was 1.7% ± 1.7% of the anteroposterior length of the brain and the estimated center located posteriorly to the center of the true AC-PC line. The angular difference between the two lines was −0.1 ± 2.7°, and thus the estimated AC-PC line was positioned just above the true AC-PC line with posterior convergence.

Validation and Comparison of the Automated Method

Accuracy of the automated estimation of the AC-PC line from PET was evaluated in seven subjects using co-registered MR images (Table 1). The horizontal and vertical displacements of the center point are 2.8% ± 0.7% of the anteroposterior length of the brain and 1.3% ± 1.6% of the brain height, which correspond to 4.2 ± 1.1 mm and 0.91 ± 1.1 mm, respectively. The relationship between the true AC-PC line and the automatically estimated AC-PC line in the PET images was effectively equivalent to the anatomical validation. The estimate AC-PC line was also positioned just above the true AC-PC line with posterior convergence.

Vertical displacements of the detected landmarks were 6.5% ± 3.5% (mean ± s.d.) for the FP, −4.8% ± 2.8% for

TABLE 1
Accuracy of the Estimated Intercommissural AC-PC Lines

Method	Angular difference[‡]	Displacement of the center	
		Horizontal[§]	Vertical[¶]
Automated	−0.6 ± 1.5	2.8 ± 0.7	1.3 ± 1.6
Manual A*	−0.4 ± 2.7	2.8 ± 1.4	−0.4 ± 1.9
Manual B[†]	0.3 ± 2.1	2.8 ± 1.3	1.3 ± 2.2

Mean ± s.d. (n = 7).
* The four landmarks were placed visually in a mid-sagittal PET plane.
[†] The direct fitting method [Friston et al. (20)].
[‡] Degrees.
[§] Percentage of the anteroposterior length of the brain.
[¶] Percentage of the brain height.

TABLE 2
Effect of Image Resolution on the Automated Estimation of the AC-PC Line

Smoothing N × N*	Angular difference[†]	Displacement of the center	
		Horizontal[‡]	Vertical[§]
3 × 3	−0.6 ± 1.7	2.7 ± 0.6	1.3 ± 1.5
5 × 5	−1.0 ± 1.8	2.6 ± 0.6	1.2 ± 1.5
7 × 7	−1.1 ± 2.2	2.6 ± 0.6	1.2 ± 1.8
9 × 9	−1.5 ± 2.0	2.6 ± 1.0	0.6 ± 1.5
11 × 11	−1.3 ± 2.1	2.2 ± 1.6	1.0 ± 1.7
13 × 13	−1.9 ± 2.4	2.1 ± 1.8	1.4 ± 1.3

Mean ± s.d. (n = 7).
* N × N pixels averaging filter.
[†] Degrees.
[‡] Percentage of the anteroposterior length of the brain.
[§] Percentage of the brain height.

the CC, 1.53% ± 4.2% for the TH and 1.8% ± 4.6% for the OP. The FP and CC tended to be detected dorsally and ventrally to the true AC-PC line, respectively.

The AC-PC lines estimated by the two manual methods also showed a minimal difference from the true AC-PC line (Table 1). When comparing the automated and the two manual methods, standard deviations of the angular difference and the displacements were smallest by the automated method. However, this was not statistically significant. No statistical differences were observed in mean values of the angular difference and the displacements by the three methods.

Effect of PET Image Resolution

With increasing image blurring, the angular difference between the true and the automatically estimated AC-PC lines gradually increased from 0.6 ± 1.5 (mean ± s.d.) to 1.9 ± 2.4° (Table 2). Although most individual angular differences were within 3.0° across the range of filters, the maximum difference of 4.1° was observed with a 13 × 13 pixel averaging filter. In this case, the angular difference without smoothing was 2.5°. However, the vertical and the horizontal displacements of the centers were stable relative to the image resolution.

Stereotactic Localization by the Automated Method

Distributions of the central sulci and parieto-occipital sulci localized by the automated estimation of the AC-PC line corresponded well to their standard locations in the stereotactic atlas (Fig. 6).

DISCUSSION

Results of the present study indicate that the AC-PC line has a nearly constant anatomical relationship with the four landmarks and can be estimated accurately and consistently in PET studies by the automated method. The relationship between true and estimated AC-PC lines in PET images was effectively equivalent to the anatomical relationship validated in MR scans. Both modalities showed posterior convergence of the two lines with mini-

mal angular differences and center displacements. In addition, the estimated AC-PC lines determined from individual PET image sets were validated in terms of localization of cerebral sulci in the stereotactic coordinate system.

Estimation of the AC-PC line from the four landmarks was very similar to that of the manual fitting method reported by Friston et al. (20). In MR scans, angular difference by our method was −0.1 ± 2.7° (mean ± s.d.) compared to their result of 0.13 ± 2.65°. The angular difference between the two methods could have been larger because their definition of the true AC-PC line was a line passing through the centers of the anterior and posterior commissures instead of the superior edge of the anterior
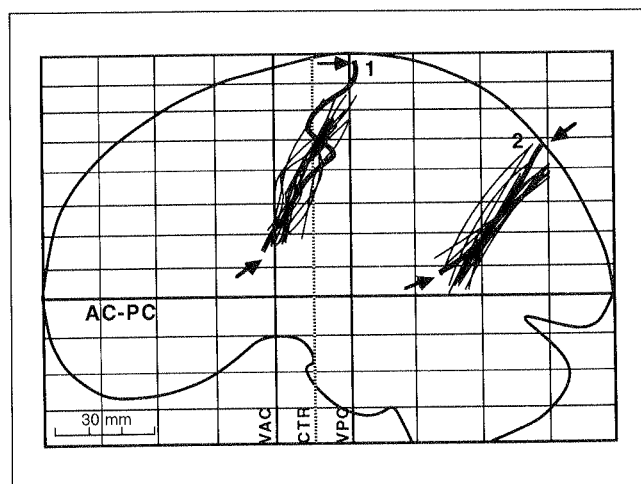

FIGURE 6. Stereotactic mapping of the central and parieto-occipital sulci. Thick lines with arrows represent standard locations of the central and parieto-occipital sulci in the stereotactic proportional system (13). 1 is the central sulci, 2 is the parieto-occipital sulci, CTR is a center line of the anterior and posterior commissures for millimetric reading (12), VAC is a vertical line passing through the anterior commissure and VPC is a vertical line passing through the posterior commissure.

commissure and the inferior edge of the posterior commissure (13) which we used in our validation. This may explain the relatively larger but nonsignificant difference of the two methods in PET-MR comparison in our study: angular difference of −0.6 ± 1.5° by the automated method and 0.3 ± 2.1° by the manual fitting method. The horizontal and vertical displacements by the automated method and the manual fitting method were approximately equal. Since MR images used in the PET-MR comparison had a slice thickness of 5 mm, this could be a source of errors in the validation. Therefore, too strict an argument cannot be made. Brain MR volume images with thinner slices would make this kind of validation even more accurate.

Potential errors in the automated method may arise due to insufficient axial sampling in PET image sets. Even with the application of a cubic spline algorithm for splice interpolation, an original PET image set of 15 slices with 6.75 mm slice separation does not permit precise determination of the vertical coordinate of each landmark. However, the estimation of the AC-PC line from the four landmarks showed minimal errors in this study possibly because the linear regression may compensate for errors in each detected landmark. The accuracy validation of the individual landmark detection indicated that the FP and CC tended to be detected dorsally and ventrally, respectively. These errors seem to be canceled out during the linear regression when estimating the AC-PC line. In fact, if estimating the AC-PC line using only the frontal pole and the occipital pole from the same data, the calculated angular difference and horizontal and vertical displacements of the center were larger: 1.4 ± 1.5°, 2.4% ± 1.0% and 4.4% ± 3.4%, respectively. Although we previously reported AC-PC line estimation from three landmarks (26), increasing the number of landmarks makes the estimation more accurate and stable.

Assuming the brain height is 70 mm and the anteroposterior length is 170 mm, a mean angular difference of −0.6° by the automated method causes displacements of approximately 0.7 mm at the top of the brain and 0.9 mm at the anterior or posterior pole of the brain in the stereotactic localization. Even the largest angular difference of 4.1° observed following the 13 × 13 pixel smoothing results in maximum displacements of only 5.0 mm at the top and 6.1 mm at the anterior or posterior pole of the brain. A mean horizontal displacement of 2.8% and a mean vertical displacement of 1.3% correspond to 4.2 mm and 0.91 mm, respectively. These small errors can be attributed to the robustness of the linear regression and are smaller than thickness of the major gyral convolutions of the brain. Because the variation in normal anatomy and functional localization are reported to be much larger than the errors introduced by stereotactic alignment with the estimated AC-PC line (20), we conclude that the errors in the automated estimation are acceptable.

The automated estimation of the AC-PC lines requires significant cortical and thalamic activities in a PET study as well as relatively normal relationship between the AC-PC line and the four landmarks. If one or more of the landmarks is shifted significantly by a focal abnormality in the brain, the estimation of the AC-PC line will be in error. Brain atrophy may also affect the accuracy of the estimation (15). We have applied the automated method to FDG PET studies of probable Alzheimer's disease patients, and the AC-PC lines were estimated accurately in 15 cases (27). This was confirmed by precise stereotactic localization of the sensorimotor cortices, where metabolic activity is relatively preserved in Alzheimer's disease and can be easily identified in a PET image. However, in one case that had a severe reduction of FDG uptake in the frontal lobe, the automated method could not identify the FP point correctly. Similar problems could occur in patients with infarction of the frontal lobe, the anterior cingulate, the thalamus or the occipital lobe. Even if the activity in the brain and the anatomical relationship of the AC-PC line with the landmarks are preserved, unexpected factors, such as unusual positioning of the head or marked extracranial activity, may disrupt the ability of the automated algorithm to detect the landmarks. Such situations may require some user interaction. The manual fitting method (20) uses different landmarks in the brain and may avoid abnormal areas which disrupt the automated method. In pathological cases, however, even if the landmarks could be detected correctly, validity of stereotaxy itself should be reconsidered. There are little data defining accuracy of stereotactic localization in pathological cases, such as severe atrophy, degenerative diseases and anatomical distortions due to focal lesions. Correlation with anatomical images (MRI, CT) would be necessary in such situations, especially areas of interest containing pathological structures.

Use of the PET image alone to orient an image set in stereotactic space has several advantages. Unlike other registration methods, this method avoids the use of additional imaging modalities such as skull x-rays (5,17), PET transmission scans (8,9) or MR scans (3–6,8,9), thus minimizing the additional expense or radiation exposure to the subject. Completely retrospective stereotactic realignment is possible with application of the current principles without the need for a special headholder or rigid frame (5,17,18). Since we validated the automated method with various smoothing filters and showed that the method works well over a large range of image resolution, it is applicable to various PET imaging procedures as long as axial sampling is comparable to or better than that used in this study. The automated method also can be applied to SPECT images with only minor modifications.

Application of PET stereotactic alignment is well suited for intersubject comparison. Because the AC-PC line is a reasonably invariant reference in neurological imaging (11,13–15,17,28), the stereotactically aligned PET images enable reproducible localization of functional information

among subjects. Our validation of the stereotactic mapping of the two major sulci indicates that the automated method works accurately for this purpose. The method also facilitates image comparison in longitudinal studies. Computation time for one subject is approximately 5 min on the workstation in our laboratory, suggesting that the method can be used routinely in clinical imaging. In neuronal activation studies with ^{15}O-water, stereotactic alignment is a key step in summation analysis proposed by Fox et al. (17,29). Subtle anatomical differences among subjects in the stereotactic space are compensated for by image smoothing in this situation. The concept of the summation also has been expanded to group by group comparison between normal and patient populations (27). When large numbers of subjects are aligned and summed in such situations, the automated method can create reproducible data with considerable time savings.

In conclusion, the intercommissural AC-PC line can be estimated accurately from internal landmarks in a PET image set. The estimation can be automated, allowing precise stereotactic alignment. As the anatomical localization of functional signals is an essential part of PET data analysis, stereotactic alignment may be of value in a wide variety of functional imaging applications.

APPENDIX

Pre-Processing of a PET Image Set

Before identifying landmarks in a PET image set, 15 reconstructed transverse slices of the original PET image are interpolated into 43 slices by a cubic spline algorithm. The original pixel size of 1.875 mm is resized by bi-linear interpolation, creating an image matrix of 128 × 128 by 43 slices with a uniform 2.25 mm voxel size. The mid-sagittal slice of the brain is determined by an automated method previously reported (30) and transformed to match with the center plane of the image matrix.

An average pixel value of the brain is calculated using a modification of the method reported by Herholz et al. (31). First, a peak pixel value is determined by the highest 5% of all pixels within the whole image set, then 25% of the peak pixel value is used as a cutoff threshold to define an approximate contour of the brain. After sorting pixels within the brain contour according to the pixel values, the middle two-thirds of the pixels are averaged to determine the average pixel value of the brain.

The approximate brain contour is re-defined by a cut-off threshold 65% of the average pixel value. Areas within this contour are filled by one. This contour image is contracted four times, expanded eight times, then contracted twice by eight-neighbor morphological erosion and dilation procedures (24), which delineates the final contour of the brain. Pixels outside of the final contour in the interpolated image are set to zero. These steps usually eliminate extraneous activity outside the brain, such as focal activity of the scalp, radioactive beads used as fiducial markers, or low activity noise in the field of view.

Detection of the Approximate CC and OP

To detect the approximate CC, the mid-sagittal slice of the brain is created by averaging resliced-sagittal slices within the middle one-sixth thickness of the brain width, thereby including the full thickness of the bilateral anterior cingulate gyri (Fig. 1A). To detect edges of the gray-white matter border and the outer surface of the brain in the averaged mid-sagittal slice, we use a combination of a smoothing filter and a Laplacian filter (22,24). First a Butterworth filter (order = 1.0, cutoff frequency = 0.078 cycles/pixel) is applied to the slice to reduce high frequency noise and blur small structures. Then, Laplacian operator is performed to extract contour information. After the Butterworth filter (order = 1.0, cutoff frequency = 0.078 cycles/pixel) is applied again to smooth small convolutions of edges, zero crossing points are searched to define edge points. The detected edges are segmented into continuous lines. Segmented lines with less than 30 pixels are discarded, creating a mid-sagittal contour image mostly which contains edges of the outer surface of the brain and gray-white matter border (Fig. 1B). The contour image is searched row by row from the right and left margins of the image matrix to determine the contour points of the outer surface. After the contour of the outer surface is detected, the most anterior point of the gray-white (GW) border is searched from top to bottom in a column, anterior to posterior, in the anterior half of the mid-sagittal contour image matrix. Then a continuous edge from the detected GW point is searched in the inferior aspect of the corpus callosum by an edge tracing technique (24). Eighteen edge pixels from the GW point usually cover the GW matter border between the inferior aspect of the anterior corpus callosum and the anterior cingulate gyrus (CC contour, Fig. 1C). These pixels are stored and used for detection of the approximate and final CC points. An approximate OP is defined as the most posterior point of the detected outer surface. An approximate CC is then defined as the most inferior point of the CC contour on a tangential line originating from the approximate OP.

Detection of the Final OP and FP

To detect the final OP and the FP, sagittal slices within the middle one-third of the brain, excluding the middle six slices which often contain interhemispheric space, are used. A cut-off threshold 90% of the average pixel value of the brain defines cortical edges of the brain in each sagittal slice. This empirically determined threshold has proved to be optimal in normal FDG and ^{15}O-water studies. To achieve fine edge sampling, the anterior and posterior cortical edge points are searched row by row from right and left margins of the sagittal image matrix with a 0.1 pixel step, using linear interpolation to detect threshold points. In each sagittal slice, the detected anterior and posterior edge points are interpolated independently by a cubic spline to create continuous functions of the edges. The OP points are detected on the interpolated posterior edge in each sagittal slice as the furthest point from the approximate CC. The final OP point is defined as a median point of the detected OP points in the vertical coordinate (Fig. 1D). Then the FP points are detected on the interpolated anterior edge in each slice as the furthest point from the final OP. The final FP point also is defined as a median point of the detected FP points in the vertical coordinate (Fig. 1D).

Definition of the Final CC and the Approximate AC-PC Line

The final CC is re-defined as the most ventral point of the previously defined CC contour on a tangential line originating from the final OP. A line is fitted to the final OP, FP and CC using simple linear regression, representing an *approximate* AC-PC line. The center of the approximate AC-PC line and the approximate AC-PC length are calculated using intersections between the line and anteroposterior edges of the brain in a mid-sagittal slice.

Definition of the TH

To detect the subthalamic point TH, we assumed that the activity of the thalamus is circular in a smoothed sagittal slice and that the peak activity of the thalamus approximately corresponds to the center of the thalamus. A mid-sagittal slice for the thalamic detection is created by averaging sagittal slices within the middle one-third of the brain width, covering the entire width of the bilateral thalami. A Butterworth filter (order = 8.0, cutoff frequency = 0.125 cycle/pixel) is applied to smooth the mid-sagittal slice. According to the predicted anatomical relationship in stereotactic space, the center of the thalamus should be located within a certain distance from the center of the AC-PC line (13). The algorithm first searches for the thalamic peak pixel (center) within a circle around the center of the approximate AC-PC line with a radius of 10% of the approximate AC-PC length. Two points from the detected thalamic center are defined as follows (Fig. 2A): assuming an imaginary circle from the thalamic center has a radius r, the first point $P1(r)$ is defined in the ventral aspect of the thalamus as the point of contact of the circle on the tangential line originating from the final OP. The second point $P2(r)$ is defined in the dorsal aspect of the thalamus, 180° opposite the point to the $P1(r)$ on the imaginary circle. The algorithm then searches for the lowest activity of the $P2(r)$ within the radius r from 1.0 to 12.0 pixels with 0.5 pixels step using linear interpolation. The lowest activity apparently represents the lateral ventricular activity above the thalamus in the averaged mid-sagittal slice. Then 70% of the thalamic peak value above the lowest ventricular value is chosen as a threshold of thalamic activity and defines the dorsal thalamic edge point $P2(r')$ (Fig. 2B). $P1(r')$ corresponding to the $P2(r')$ is determined as the subthalamic point TH (Fig. 2B). The 70% threshold was empirically determined from normal FDG and ^{15}O-water images.

REFERENCES

1. Mazziotta JC. Physiologic neuroanatomy: new brain imaging methods present a challenge to an old discipline. *J Cereb Blood Flow Metab* 1984; 4:481–483.
2. Correia JA. Registration of nuclear medicine images. *J Nucl Med* 1990; 31:1227–1229.
3. Meltzer CC, Bryan RN, Holcomb HH, et al. Anatomical localization for PET using MR imaging. *J Comput Assist Tomogr* 1990;14:418–426.
4. Mosskin M, Ericson K, Hindmarsh T, et al. Positron emission tomography compared with magnetic resonance imaging and computed tomography in supratentorial gliomas using multiple stereotactic biopsies as reference. *Acta Radiol* 1989;30:225–232.
5. Evans AC, Beil C, Marrett S, Thompson CJ, Hakim A. Anatomical-functional correlation using an adjustable MRI-based region of interest atlas with positron emission tomography. *J Cereb Blood Flow Metab* 1988; 8:513–530.
6. Evans AC, Marrett S, Torrescorzo J, Ku S, Collins L. MRI-PET correlation in three dimensions using a volume-of-interest (VOI) atlas. *J Cereb Blood Flow Metab* 1991;11:A69–78.
7. Levin DN, Pelizzari CA, Chen GT, Chen CT, Cooper MD. Retrospective geometric correlation of MR, CT, and PET images. *Radiology* 1988;169: 817–823.
8. Pelizzari CA, Chen GT, Spelbring DR, Weichselbaum RR, Chen CT. Accurate three-dimensional registration of CT, PET, and/or MR images of the brain. *J Comput Assist Tomogr* 1989;13:20–26.
9. Vannier MW, Gayou DE. Automated registration of multimodality images. *Radiology* 1988;169:860–861.
10. Matsui T, Hirano A. *An atlas of the human brain for computerized tomography*. New York: Igaku-Shoin; 1978.
11. Tokunaga A, Takase M, Otani K. The glabella-inion line as a baseline for CT scanning of the brain. *Neuroradiology* 1977;14:67–71.
12. Talairach J, Szikla G, Tournoux P, et al. *Atlas d'anatomie stéréotaxique du télencéphale*. Paris: Masson; 1967.
13. Talairach J, Tournoux P. *Co-planar stereotaxic atlas of the human brain*. New York: Thieme Medical Publishers; 1988.
14. Takase M, Tokunaga A, Otani K, Horie T. Atlas of the human brain for computed tomography based on the glabella-inion line. *Neuroradiology* 1977;14:73–79.
15. Fox PT, Kall B. Stereotaxy as a means of anatomical localization in physiological brain images proposals for further validation. *J Cereb Blood Flow Metab* 1987;7:S18–20.
16. Bohm C, Greitz T, Kingsley D, Berggren BM, Olsson L. Adjustable computerized stereotaxic brain atlas for transmission and emission tomography. *AJNR* 1983;4:731–733.
17. Fox PT, Perlmutter JS, Raichle ME. A stereotactic method of anatomical localization for positron emission tomography. *J Comput Assist Tomogr* 1985;9:141–153.
18. Zhang J, Levesque MF, Wilson CL, et al. Multimodality imaging of brain a structures for stereotactic surgery. *Radiology* 1990;175:435–441.
19. Strother S, Perlmutter JS. Headholders for functional brain imaging. *J Cereb Blood Flow Metab* 1987;7:S16–S18.
20. Friston KJ, Passingham RE, Nutt JG, Heather JD, Sawle GV, Frackowiak RS. Localisation in PET images. direct fitting of the intercommissural (AC-PC) line. *J Cereb Blood Flow Metab* 1989;9:690–695.
21. Spinks TJ, Jones T, Gilardi MC, Heather JD. Physical performance of the latest generation of commercial positron scanner. *IEEE Trans Nucl Sci* 1988;35:721–725.
22. Pietrzyk U, Herholz K, Heiss WD. Three-dimensional alignment of functional and morphological tomograms. *J Comput Assist Tomogr* 1990;14: 51–59.
23. Zar JH. *Biostatistical analysis*. New Jersey: Prentice-Hall; 1984.
24. Rosenfeld A, Kak AC. *Digital picture processing*. New York: Academic Press; 1976.
25. Steinmetz H, Furst G, Freund HJ. Cerebral cortical localization: application and validation of the proportional grid system in MR imaging. *J Comput Assist Tomogr* 1989;13:10–19.
26. Minoshima S, Berger KL, Lee KS, Taylor SF, Mintun MA. Automated detection of the intercommissural (AC-PC) line for stereotactic registration of PET images [Abstract]. *J Nucl Med* 1991;32:966.
27. Minoshima S, Berger KL, Koeppe RA, Frey KA, Mintun MA, Kuhl DE. Automated registration and standardization of functional brain images: new diagnostic tool for brain PET study. *Radiology* 1991;181(P):101.
28. Vanier M, Lecours AR, Ethier R, et al. Proportional localization system for anatomical interpretation of cerebral computed tomograms. *J Comput Assist Tomogr* 1985;9:715–724.
29. Fox PT, Mintun MA, Reiman EM, Raichle ME. Enhanced detection of focal brain responses using intersubject averaging and change-distribution analysis of subtracted PET images. *J Cereb Blood Flow Metab* 1988;8: 642–653.
30. Minoshima S, Berger KL, Lee KS, Mintun MA. An automated method for rotational correction and centering of three-dimensional functional brain images. *J Nucl Med* 1992;33:1579–1585.
31. Herholz K, Pawlik G, Wienhard K, Heiss WD. Computer assisted mapping in quantitative analysis of cerebral positron emission tomograms. *J Comput Assist Tomogr* 1985;9:154–161.